Eur. Phys. J. B **51**, 111–118 (2006)
DOI: 10.1140/epjb/e2006-00186-9

THE EUROPEAN PHYSICAL JOURNAL B

Cooperative motions in a finite size model of liquid silica: an anomalous behavior

V. Teboul[a]

Laboratoire des Propriétés Optiques des Matériaux et Applications, CNRS UMR 6136, Université d'Angers, 2 Bd Lavoisier, 49045 Angers Cedex, France

Received 1st July 2005 / Received in final form 15 October 2005
Published online 31 May 2006 –

Abstract. Finite size effects on dynamical heterogeneity are studied in liquid silica with Molecular Dynamics simulations using the BKS potential model. When the system size decreases relaxation times are found to increase in accordance with previous results in finite-size simulations and confined liquids. It has been suggested that this increase may be related to a modification of the spatially heterogeneous dynamics in confined liquids. In agreement with this hypothesis we observe a decrease of the spatially heterogeneous dynamics when the size decreases. The spatially heterogeneous dynamics is usually characterized by the dynamical aggregation of the most or the least mobile atoms. However we find that the decrease of the dynamical aggregation associated to the least mobile atoms is much more important than the decrease associated to the most mobile atoms when the size decreases. This result associated with a slowing down of the liquid is surprising as it is expected that the dynamical aggregation of the least mobile atoms should increase the slowing down of the liquid dynamics. The decrease of the heterogeneous behaviour is also in contradiction with the increase of the spatially heterogeneous dynamics observed in liquids confined inside nanopores. However, an increase of the non-Gaussian parameter appears both for the confinement inside nanopores and for the finite size simulations. As the non-Gaussian parameter is usually associated with the heterogeneous dynamics, the increase of the non-Gaussian parameter together with a decrease of the spatially heterogeneous dynamics is also surprising.

PACS. 61.43.Fs Glasses – 64.70.Pf Glass transitions – 66.10.Cb Diffusion and thermal diffusion

Introduction

The existence of cooperative molecular or atomic motions in supercooled glass-forming liquids is commonly invoked [1–3] as the likely explanation for the dramatic increase of the viscosity as the liquid is cooled toward its glass transition. The existence of spatially heterogeneous dynamics in supercooled liquids has been reported either experimentally near the glass transition temperature or with molecular dynamics simulations well above this temperature [2,3]. From MD simulations these heterogeneities are usually characterized by an aggregation of the most mobile atoms [2–12] and of the least mobile atoms [2,12]. Whether dynamical heterogeneities are partly the origin of the strange behavior of glass-forming liquids or are only an interesting consequence of it, is however still a matter of conjecture. And whether the cooperative motions expected by some theories [1] may be associated with the cooperative motions of the heterogeneous dynamics is also still a matter of debate.

When the liquid is confined inside a pore a few nanometers across the cooperative motions will not be able to extend over a distance larger than the pore size. As a consequence, a modification of the dynamical properties is expected which may give information on the nature of the cooperative motions [2,3,9,13,14]. Indeed, the physical properties of the liquid change drastically with confinement [9,13,15,16]. However, if these changes originate partly from finite size effects, anisotropy and surface effects also play an important role [13,14]. In other words, liquids confined inside nanopores are subject to different contributions: a strong surface contribution and a finite-size contribution are both present [13,15]. Surface contributions predominate near the surface of the pore but decrease rapidly as the distance from the surface increases [9,13,15]. On the contrary, finite-size effects do not depend on the distance from the surface of the pore. As a result when pore diameters are large enough to eliminate surface effects and small enough for non negligible finite size effects, finite-size effects are expected to predominate in the center of the pore. In agreement with this viewpoint, it has been observed for various liquids that the alpha relaxation times may be fitted by the sum of a decreasing exponential from the pore surface (surface effect) and a constant part (finite-size effect) [13].

In this context, a direct investigation of finite-size effects may help to separate the different contributions of the above-mentioned mechanisms that appear when a

[a] e-mail: victor.teboul@univ-angers.fr

liquid is confined inside a pore. These studies may also give indirect information on the size of cooperative motions in the liquid. More generally, an investigation of finite-size effects may give information on the size of the phenomena of physical importance for the relaxation mechanisms in the liquid. A simple method, which seems not to be affected by surface effects is to use a finite cubic box of size L with periodic boundary conditions (p.b.c.). Confined liquids dynamics displays an increase or a decrease of relaxation times due to surface contributions [15] depending on the roughness of the surface. However, for finite boxes with p.b.c simulations, when the size L decreases, it has been found [17–19] in various liquids, including silica [18,19] that relaxation times increase. This increase was found to be larger for strong liquids [19] like silica than for fragile liquids [20]. The reason for this increase is however still unclear. It has been suggested that this increase may be related to a modification of the spatially heterogeneous dynamics in confined liquids [17]. In agreement with this hypothesis we observe a decrease of the dynamical heterogeneities associated with the most and the least mobile atoms when the size L decreases. However, we find that the decrease of the dynamical aggregation associated with the least mobile atoms is much more important than the decrease associated with the most mobile atoms. This result of a slowing down of the liquid is surprising as it was expected that the dynamical aggregation of the least mobile atoms would increase the slowing down of the liquid dynamics. The decrease of the heterogeneous behaviour is also in contradiction with the increase of the heterogeneities observed in liquids confined in nanopores [9]. Meanwhile an increase of the non-Gaussian parameter appears both in nanopore confinement and in the finite size simulations. As the non-Gaussian parameter is usually associated with dynamical heterogeneities, the increase of the non-Gaussian parameter together with a decrease of dynamical heterogeneity is also surprising. Finally, it has been found previously in silica [21] that the Kohlrausch-Williams-Watts (KWW) parameter associated with the intermediate scattering function does not show significant finite-size effects. When compared to homogeneous dynamics, heterogeneous dynamics will increase [2,3,9] the stretching of the correlation functions, and so the KWW parameter (or stretching parameter) has been related by some authors to the heterogeneous dynamics [2,3]. From this viewpoint a decrease of the heterogeneity will then increase this parameter (i.e. decrease the stretching). That the KWW parameter doesn't show significant finite-size effects shows that another cause compensates the decrease of the heterogeneity for the stretching parameter evolution.

Calculation

Our simulations use the Verlet algorithm [22] to solve the equations of motions with the BKS potential [23,24]. This potential was reported to be one of the most realistic potentials in silica for the study of the dynamical properties [25]. A very short range repulsive part was added, as described by Guissani and Guillot [24], in order to eliminate the possible short range divergence of this potential. The reaction field method [22] was employed to take into account long-range electrostatic interactions under the same conditions as described in reference [26]. The reaction field method increases the long range screening of the potential function and leads to a slight decrease of the diffusivity in comparison with the original model. This modification leads to diffusion coefficients for the oxygen and silicon atoms that are in slightly better agreement with the experimental data [26]. This modification of the potential function produces [26] activations energies of 4.72 eV for the oxygen atoms and 5.36 eV for the silicon atoms, which is also in relatively good agreement with the experimental data of 4.7 eV [27] and 6.0 eV [28].

The time step was chosen equal to 10^{-15} s. The system is heated to a temperature of 7000 K to ensure homogenization. It is then cooled to the different temperatures under study using a Berendsen thermostat [29]. The simulations are then aged by 20 nanoseconds before any treatment. This very large aging time has been found to be necessary in order to ensure stabilization at the temperature under study. Here, the aging time is evaluated from the decrease of various correlation functions to zero and from the mean square displacement evolution to a pure diffusive behaviour. The absence of a constant long time drift in the studied correlation functions is then verified during the treatment. In order to study the size effects we have used various box sizes ranging from 20 Å to 50 Å in width, i.e. from 576 to 9000 atoms. The density was set to a constant of 2.3 g/cm^3 in our simulations. The simulations are performed at constant temperature in the (N, V, T) ensemble, below the MCT critical temperature for this model $T_C = 3330$ K.

In the Markovian approximation, the self-part of the Van Hove correlation function $G_s(r,t)$ has a Gaussian form. This function is defined by

$$G_s(\mathbf{r},t) = \left\langle \frac{1}{N}\sum_{i=1}^{N} \delta\left(\mathbf{r} + \mathbf{r}_i(t_0) - \mathbf{r}_i(t+t_0)\right)\right\rangle \quad (1)$$

where $4\pi r^2 G_s(r,t)$ represents the probability for a particle to be at time $t+t_0$ at a distance r from its position at time t_0. Departure from this Gaussian form has been found in various glass forming liquids and is thought to be due to dynamical heterogeneities. Such deviations are usually characterized by the Non-Gaussian parameter:

$$\alpha_2(t) = 3\left\langle r^4(t)\right\rangle / 5\left\langle r^2(t)\right\rangle^2 - 1 \quad (2)$$

where $\langle r^2(t)\rangle$ is the mean square displacement.

We define the mobility $\mu_{i,t0}(t)$ of atom i at time t_0 within a characteristic time t, by the relation [10,30]:

$$\mu_{i,t0}(t) = \left|\mathbf{r}_i(t+t_0) - \mathbf{r}_i(t_0)\right| / \left(\left\langle r^2(t)\right\rangle\right)^{0.5}. \quad (3)$$

The mobility of atom i at time t_0 is then defined as the normalized displacement of atom i during a time t. In the rest of the discussion, we will omit the time t_0 which will disappear in the mean statistical values. We then select

atoms of high or low mobility for the calculation of the dynamical heterogeneity. This selection is then dependent on the time t chosen for the definition of the mobility $\mu_i(t)$. Here, we define the 6 percent of atoms with largest mobility as most mobile (MM), and as least mobile (LM) the 6 percent of atoms with lowest mobility. We then select atoms of high and low mobility for the calculation of the dynamical heterogeneity. This selection of atoms of high and low mobility depends on the time t chosen in the definition of the mobility. We define here the function [10,12]:

$$A^+(r,t) = G_{mm(t)}(r,0)/G(r,0) - 1. \quad (4)$$

In this formula $G_{mm(t)}(r,0)$ is the radial distribution function between the most mobile oxygen atoms, and $G(r,0)$ is the mean radial distribution function between two oxygen atoms. $A^+(r,t)$ gives a measure of the correlation increase between mobile atoms. Similarly we define $A^-(r,t)$ for the least mobile atoms. In order to eliminate infinite values, we define $A^{+/-}(r,t) = 0$ when $G(r,0) < 0.05$. This definition implies that $A^{+/-}(r,t)$ is only meaningful above a certain cut-off distance defined by $G(r,0) > 0.05$. This cut-off distance is here 2.2 Å for oxygen atoms.

We then define the integrals $I^{+/-}(t)$ of the functions $A^{+/-}(r,t)$ by [10,12]:

$$I^{+/-}(t) = \int_0^{R_C} A^{+/-}(r,t).4\pi r^2 dr. \quad (5)$$

This definition differs from the definition in reference [12] by a factor N/V. In our simulations $A^{+/-}(r,t)$ is only defined for $r < L/2$, and the box size L evolves from 20 to 50 Å. In order to eliminate direct truncation effects on the evolution of the function $I^{+/-}(t)$ with the size of the box, we have truncated the integral in the following calculations at a cut-off value $R_C = 10$ Å which corresponds to the shortest $L/2$ value investigated. In our notations, the functions $A^-(r,t)$ and $I^-(r,t)$ correspond to the least mobile atoms while functions $A^+(r,t)$ and $I^+(t)$ correspond to the most mobile atoms. The functions $A^{+/-}(r,t)$ represent the correlation increase between atoms of approximately the same mobility, and distant of r. Thus, the functions $I^{+/-}(t)$ represent the global increase of the correlation between atoms of high (I^+) or low (I^-) mobility. Following reference [12] we will name the function $I^{+/-}(t)$: Intensity of the aggregation. We finally define the characteristic times t_+ and t_- as the times that correspond to the maximum of the functions $I^+(t)$ and $I^-(t)$ respectively.

Results

Figure 1 shows the non-Gaussian parameter $\alpha_2(t)$ (2) and the mean square displacement $\langle r^2(t)\rangle$ of oxygen atoms, for various system sizes L ranging from 20 Å to 50 Å. We observe in Figure 1 an increase of the non-Gaussian parameter when the system size L decreases. As usual in glass-forming liquids, this increase of the non-Gaussian parameter is observed together with a slowing down of the dynamics of the liquid [13]. This slowing down has been reported previously by different authors [18,19]. In particular, it has been demonstrated [19] that the short time dynamics (for $t < 0.1$ ps) was not affected by the system size modification while the long time dynamics slows down. In order to illustrate this evolution, in the inset of Figure 1 we have plotted the mean square displacement evolution with the system size at a temperature of 3100 K. We observe in the inset that the modification of the mean square displacement appears around the end of the plateau time regime. This result suggests that the system size modification affects the probability for an atom to escape the cage constituted by its neighbours [31]. Because dynamical heterogeneity is also at a maximum around the end of the plateau time regime, this result agrees well with an interpretation of size effects resulting from a modification of the spatially heterogeneous dynamics [17]. This result may be seen clearly in Figure 1 which displays the non-Gaussian parameter time evolution together with the

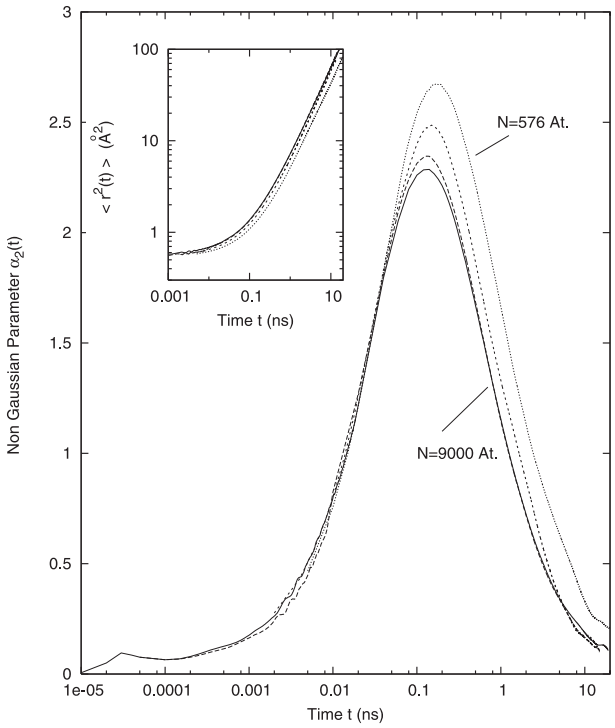

Fig. 1. Non Gaussian parameter for oxygen atoms in liquid silica for different system sizes. The temperature is 3100 K. From bottom to top: continuous line: $L = 50$ Å ($N = 9000$ atoms), short dashed line $L = 40$ Å ($N = 4608$ atoms), bold dashed line: $L = 25$ Å ($N = 1125$ atoms), dotted line: $L = 20$ Å ($N = 576$ atoms). The Non-Gaussian parameter decreases when the size of the box increases. Inset: Mean square displacement for oxygen atoms (Å^2) in liquid silica for different system sizes. The temperature is 3100 K. From top to bottom: Continuous line: $L = 50$ Å ($N = 9000$ atoms), short dashed line (superimposed on the continuous line) $L = 40$ Å ($N = 4608$ atoms), bold dashed line: $L = 25$ Å ($N = 1125$ atoms), dotted line: $L = 20$ Å ($N = 576$ atoms). $\langle r^2(t)\rangle$ is plotted on a logarithmic scale.

mean square displacement time evolution, if we use the non-Gaussian parameter as a measure of the dynamical heterogeneity. In Figure 1 we observe indeed that the maximum of the non-Gaussian parameter corresponds to the time regime where the mean square displacement modification begins. On the other hand, the observed increase of the non-Gaussian parameter seems to be in contradiction with the expected decrease of the dynamical heterogeneity when the system size decreases.

We also observe in Figure 1 that the non-Gaussian parameter increases strongly as the half system size $(L/2)$ decreases below 12.5 Å. In parallel we observe that the mean square displacement also changes strongly when the same system size is crossed. These results suggest that the size of cooperative motions at the temperature under study (3100 K) is around 12.5 Å. The characteristic time t^* which corresponds to the maximum of the non-Gaussian parameter also increases for the same system size, but only slightly as seen in Figure 1. We note that this increase of t^* is much weaker than that observed due to a decrease in temperature corresponding to the same maximum value of the non-Gaussian parameter. A slowing down of the dynamics associated with an increase of the non-Gaussian parameter may also be observed when supercooled liquids are confined inside pores a few nanometers across [13]. However, the increase of the non-Gaussian parameter and the dynamical slowing down are much larger in nanopore confinement than is observed here for the same sizes of confinement. In agreement with previous studies of various surfaces contributions [15], this result suggests that the slowing down of the dynamics and the associated increase of the non-Gaussian parameter in nanopores is due largely to the interaction with the surface of the pore.

In supercooled liquids the non-Gaussian parameter (2) usually increases when the temperature decreases and this evolution is associated with an increase of the dynamical heterogeneity. The time evolution of the non-Gaussian parameter corresponds also to the time evolution of dynamical heterogeneity. These behaviours have been observed in particular in liquid silica [8,10] and in various glass-formers. For these reasons among others, in glass-forming liquids the non-Gaussian parameter is usually associated with the presence of dynamical heterogeneity. We will now investigate the evolution of the dynamical heterogeneity when the system size decreases. When the system size decreases, the dynamical aggregation will not be able to extend over distances larger than the system size, and this truncation effect leads to a decrease in the dynamical heterogeneity. In other words, a decrease of R_c due to the decrease of the box size, in equation (5) leads to a decrease of $I(t)$, because $A(r,t)$ is positive. Then the question of another non-trivial effect on the heterogeneity arises. We will focus our attention on this question (i.e. on the evolution of the heterogeneity with a fixed cut-off R_c) in the forthcoming paragraphs, followed by a further study of the direct truncation effect.

Figures 2a and 2b show the functions $A^+(r,t)$ and $A^-(r,t)$ versus distance r for different values of time t, including the time (t_+ or t_-) corresponding to the maximum

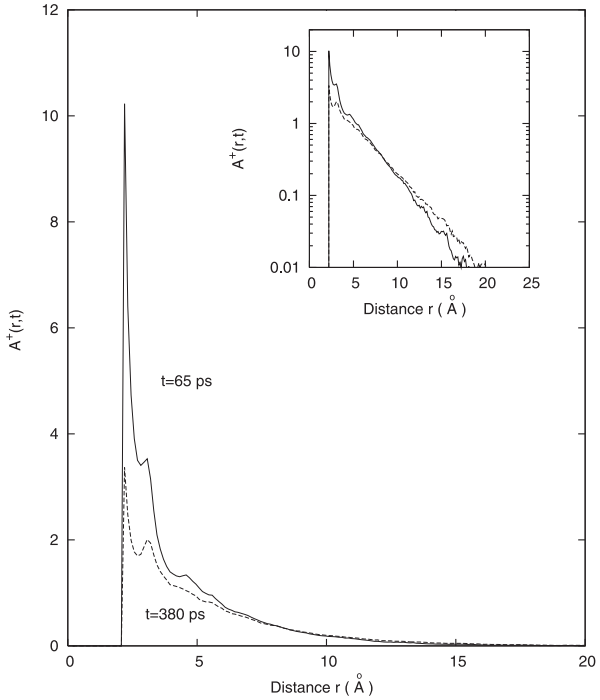

Fig. 2. (a) Function $A^+(r,t) = G_{mm(t)}(r,0)/G(r,0) - 1$ for $t = t_+ = 65$ ps (continuous line) corresponding to the maximum of the function $I^+(t)$ (second peak) and for $t = 380$ ps (dashed line) corresponding to the third peak of the function $I^+(t)$. The temperature is 3100 K. (b) Function $A^-(r,t) = G_{lmlm(t)}(r,0)/G(r,0) - 1$ for $t = t_- = 2500$ ps (continuous line) corresponding to the maximum of the function $I^-(t)$ and for $t = 380$ ps (dashed line). The temperature is 3100 K. Inset: same curves on a Logarithmic scale.

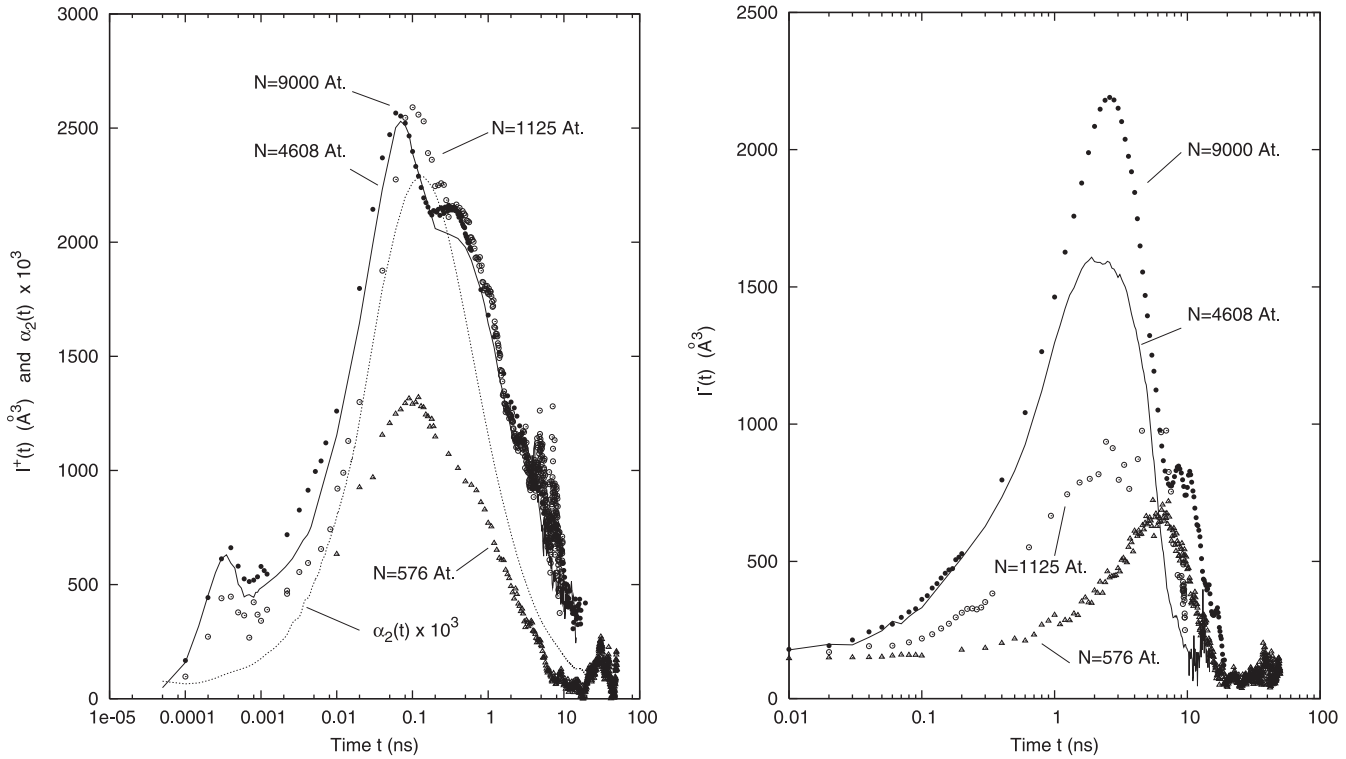

Fig. 3. (a) Function $I^+(t) = \int_0^{R_C} A^+(r,t) \cdot 4\pi r^2 dr$ with $R_c = 10$ Å, for the oxygen atoms. This definition differs from the definition in reference [12] by a factor N/V. Different system sizes are considered: Full circles: $L = 50$ Å ($N = 9000$ atoms), continuous line $L = 40$ Å ($N = 4608$ atoms), empty circles: $L = 25$ Å ($N = 1125$ atoms), triangles: $L = 20$ Å ($N = 576$ atoms). The non-Gaussian parameter (dotted line) multiplied by a factor 1000 and corresponding to the largest size investigated ($L = 50$ Å) is plotted for comparison. The temperature is 3100 K. (b) Function $I^-(t) = \int_0^{R_C} A^-(r,t) \cdot 4\pi r^2 dr$ with $R_c = 10$ Å, for the oxygen atoms. Different system sizes are considered: full circles: $L = 50$ Å ($N = 9000$ atoms), continuous line $L = 40$ Å ($N = 4608$ atoms), empty circles: $L = 25$ Å ($N = 1125$ atoms), triangles: $L = 20$ Å ($N = 576$ atoms). The temperature is 3100 K.

of the function $I^{+/-}(t)$ (continuous lines). In the inset, the same functions are plotted on a logarithmic scale in order to show more accurately the long range correlations. The inserts in Figure 2 show that the $A^{+/-}(r,t)$ functions evolution versus r follow a pure exponential decay. The functions $A^-(r,t)$ (Fig. 2b inset) display oscillations due to an increase of the structural order for the least mobile atoms (maxima/minima of the function $G_{lmlm}(r,0)$ are higher/smaller than maxima/minima of $G(r,0)$ leading to oscillations in $A^-(r,t)$). These oscillations do not appear for the aggregation of the most mobile atoms $A^+(r,t)$. We also observe in Figure 2 that the size of the aggregates is larger for atoms of low mobility than for atoms of high mobility as the slope of the exponential decay is larger for $A^+(r,t)$ than for $A^-(r,t)$. Atoms of high mobility are however more correlated at short range than atoms of low mobility. Indeed, we see in Figure 2 that the maximum of $A^+(r,t_+)$ is around 10 for the first neighbour position compared to $A^-(r,t_-) = 2.6$ at the same position. We also observe in the inset of Figure 2a an increase of the long range correlation when the time increases (for $r > 8$ Å the dashed line curve that corresponds to $t = 380$ ps is higher than the continuous line that corresponds to $t = t_+ = 65$ ps). This increase will lead to a secondary maximum value in the integral $I^+(t)$ (Fig. 3a) due to the $4\pi r^2$ factor which increases the importance of long range distances in $I^+(t)$. The origin of this increase of the long range correlations in $A^+(r,t)$ and then of this secondary maximum of $I^+(t)$ is however still unclear. If an increase of the long range part in $A^+(r,t)$ with time may be expected from the diffusion process we would expect that the decrease of the short range part will compensate this effect leading to a global decrease of $I^+(r,t)$. As a tentative explanation we suggest that this increase may originate in the merging of different aggregates as their size increases before their total disappearance.

Figures 3a and 3b show the evolution of the dynamical heterogeneity when the system size decreases. In this calculation, in order to eliminate the simple truncation effect mentioned above on the size of the heterogeneities, we have used the same cut-off value $R_c = 10$ Å in the calculation of the intensities $I^+(t)$ or $I^-(t)$ (5) for the different system sizes. This value of R_c corresponds to the half-size of the shorter system considered here. We observe that even without the truncation effect, the dynamical heterogeneities decrease when the system size decreases. Surprisingly, this decrease is associated with an increase of the non-Gaussian parameter. This result is amazing if we

suppose that the non-Gaussian evolution of the Van Hove correlation function (1) that results in a non-Gaussian parameter different from zero, is entirely due to the heterogeneity in displacements. A decrease of the heterogeneous motion will then lead to a decrease of the non-Gaussian parameter contrary to what is observed here. This result suggests that the non-Gaussian behaviour is not only due to the presence of the dynamical heterogeneity but that other causes are also involved. We note that in the case of a liquid confined in a pore the opposite result is observed [9]. In this case, the heterogeneity increases together with the non-Gaussian parameter when the liquid is confined. This increase of the heterogeneous motion is however maximum around the pore surface and may then be related to surface effects.

In Figure 3a we show for comparison the non-Gaussian parameter corresponding to the largest system size investigated ($L = 50$ Å) i.e. to the liquid dynamics without finite-size effects. Figure 3a shows that the Non Gaussian parameter follows the main time evolution of the intensity $I^+(t)$ of the heterogeneity (aggregation of the most mobile atoms). This result suggests a relation between the non-Gaussian parameter and the dynamical heterogeneity as observed previously in supercooled water [12]. We also observe in Figure 3a different maxima in the intensity of the heterogeneity $I^+(t)$. These maxima do not appear for the intensity $I^-(t)$ associated with the aggregation of atoms of low mobility in Figure 3b. The first peak corresponds to short times (around 0.4 ps). This time regime corresponds to the very beginning of the plateau time regime observed in the mean square displacement. As others authors have noted [32], we also observe a peak in the Non Gaussian parameter but for a shorter time scale, this peak may be related to the Si-O bond breaking process. The second peak in Figure 3a corresponds approximately to the maximum of the non-Gaussian parameter. It corresponds to the maximum of the short-range correlation for the dynamical aggregation as seen in Figure 2a. The third peak corresponds to an increase of the number of atoms correlated at longer distances as discussed before (Fig. 2a inset). This third peak is deeply affected by the cut-off distance R_c. When R_c decreases this peak decreases sharply, as seen in Figures 4a and 4b. This result suggests that long range correlations are partly at the origin of this peak. This peak is not observed in supercooled water [12], a liquid which presents however, a number of similarities with silica.

We observe in Figure 3a that size effects on the aggregation of the most mobile atoms are weak, for system sizes above or equal to 12 Å, when the direct truncation effects are removed. The size effects begin then to be important for sizes shorter than or around 10 Å. On the contrary, Figure 3b shows that size effects appear around 20 Å for the dynamical aggregation associated with atoms of low mobility. The heterogeneity associated with atoms of low mobility appears then to be more sensitive to finite size effects, independently of the direct truncation effect associated with the size of the heterogeneity. A comparison between Figures 3a and 3b shows that the aggregation of the least mobile atoms decreases much faster with the system size than the aggregation of the most mobile atoms. If for $N = 9000$ atoms $I^+(t)$ and $I^-(t)$ are roughly equal, for $N = 576$ atoms the intensity $I^+(t)$ is approximately twice the intensity $I^-(t)$, as seen in Figures 3a and 3b. In both cases however, the decrease accelerates abruptly for $N = 1125$ atoms, i.e. a half box size of 12.5 Å. This size corresponds approximately to the size of the heterogeneities at this temperature (3100 K) as seen in Figures 2a and 2b. We notice however that for atoms of low mobility ($I^-(t)$ Fig. 3b) the decrease is progressive before accelerating for $N = 1125$ atoms, while atoms of high mobility ($I^+(t)$ Fig. 3a) show a different behaviour. There is no size effects (if we except the simple truncation effect that will be discussed later) as long as $N > 1125$ atoms while the intensity decreases sharply for N shorter than 1125 atoms.

We will now study the direct truncation effect on the intensity of the dynamical heterogeneity. Figures 4a and 4b show the effect of the truncation of function $A^{+/-}(r,t)$ with different cutoff values on the intensity $I^{+/-}(t)$ for the most mobile atoms (Fig. 4a) and the least mobile atoms (Fig. 4b). For the largest cutoff ($R_c = 12$ Å) we observe that the intensities $I^+(t)$ and $I^-(t)$ are roughly equal. This equality between the intensities of two sorts of heterogeneities that are physically very different has been observed previously in supercooled water [12]. Indeed, the most mobile atoms shows string like motion while the least mobile atoms do not [10]; the least mobile atoms are structurally more ordered in the bulk in contrast to the most mobile atoms; and different characteristic times are observed. Figures 4a and 4b show that the intensity decrease with the cutoff R_c is more rapid for the aggregation of atoms of low mobility (Fig. 4b) than for the aggregation of atoms of high mobility (Fig. 4a). In both cases (Figs. 4a and 4b) this decrease is continuous. As long as truncation effects are concerned, we do not see any acceleration of the decrease of $I^{+/-}(t)$ versus the cutoff value R_C for specific values of R_C. Figure 4a shows that the secondary peak disappears for $R_C = 5$ Å or less. This is in accordance with a long range effect origin for this peak. Figure 4a also shows that the intensity of the first small peak stays constant for R_C larger than 8 Å then decreases sharply for R_C smaller than 5 Å. This peak has been attributed to a collective vibrational mode [11]. This result shows that the associated correlation range corresponds to a radius of 5 Å (i.e. the second neighbour distance).

Finally, Figures 3 and 4 show that the decrease of $I^-(t)$ with the system size decrease is larger than the decrease of $I^+(t)$. This result is surprising as it is associated with a slowing down of the dynamics. If the modification of the dynamics is due to a modification of the spatially heterogeneous dynamics then we expect that a slowing down of the dynamics will be associated with a decrease of the dynamical aggregation of the most mobile atoms or an increase of the dynamical aggregation of the atoms of low mobility. This result suggests that the modification of the dynamics here is only partly due to the dynamical heterogeneity or alternatively that the atoms of low mobility

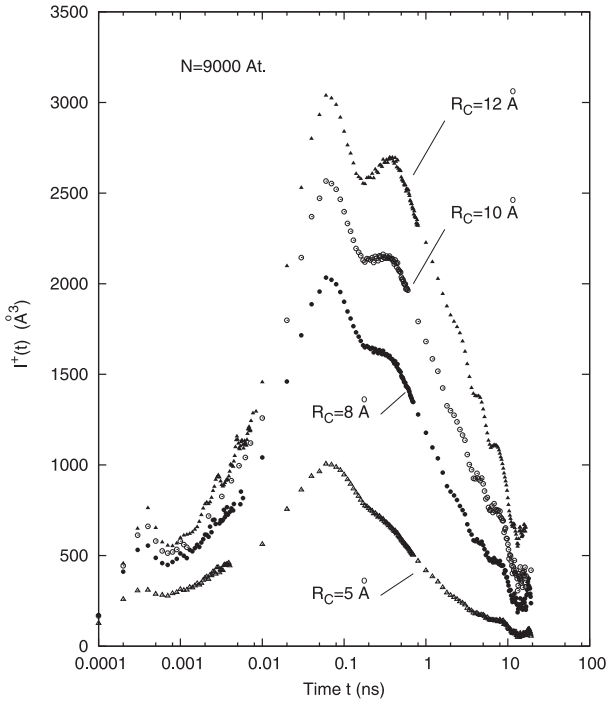

(a)

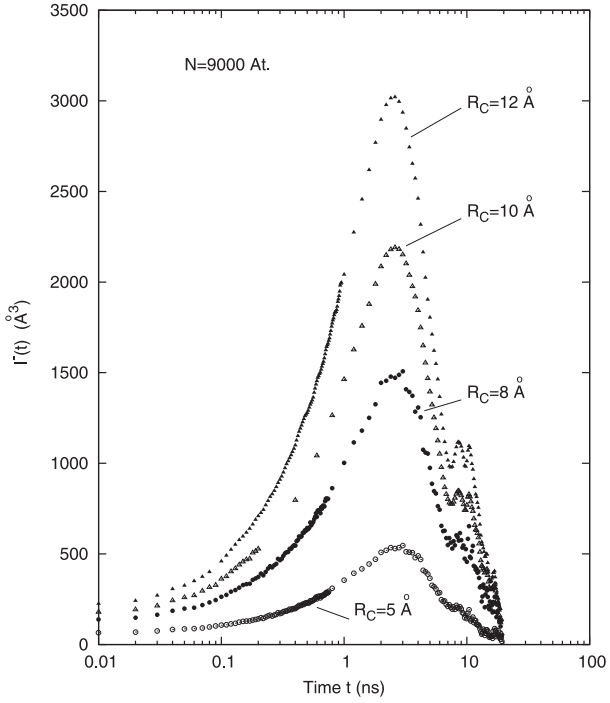

(b)

Fig. 4. (a) Function $I^+(t) = \int_0^{R_C} A^+(r,t).4\pi r^2 dr$ for the oxygen atoms and for different values of the cutoff radius R_C ranging from 12 to 5 Å. The system size is the same for all curves: $L = 50$ Å corresponding to $N = 9000$ atoms. The temperature is 3100 K. (b) Function $I^-(t) = \int_0^{R_C} A^-(r,t) \cdot 4\pi r^2 dr$, for the oxygen atoms and for different values of the cutoff radius R_C ranging from 12 to 5 Å. The system size is the same for all curves: $L = 50$ Å corresponding to $N = 9000$ atoms. The temperature is 3100 K.

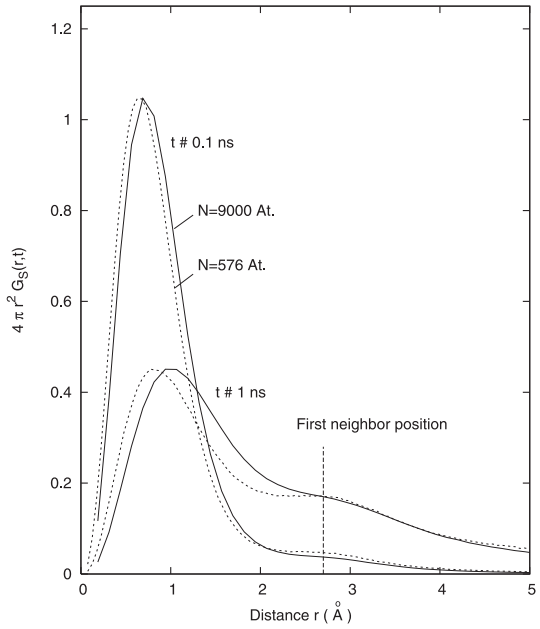

Fig. 5. Van Hove correlation function $G_s(r,t)$ versus distance r, for the largest and smallest size investigated. Dashed lines: $L = 20$ Å ($N = 576$ atoms) with $t = 0.2$ ns (left hand side) and $t = 1.75$ ns (right hand side); Continuous lines: $L = 50$ Å ($N = 9000$ atoms) with $t = 0.1$ ns (left hand side) and $t = 1$ ns (right hand side). The small dashed line shows the position of the first oxygen neighbour.

have a much weaker effect on the dynamics than the atoms of high mobility.

In order to answer this question we will now investigate the evolution of the self Van Hove correlation function (1) for different system sizes. Figure 5 shows the Van Hove $G_s(r,t^*)$ multiplied by a factor $4\pi r^2$ and applied to the system sizes of $L/2 = 10$ Å and $L/2 = 25$ Å. We observe in Figure 5 the tail of the function, which corresponds to atoms of large mobility, and which has been usually associated with dynamical heterogeneity. Due to the presence of this tail, the Van Hove correlation function cannot be a Gaussian and the non-Gaussian parameter is then different from zero.

We observe in Figure 5 the self Van Hove correlation functions corresponding to two different box sizes at two different times. The smaller box results are displayed with dashed lines and the larger box results with continuous lines. A short dashed line has been added in order to visualize the first neighbour distance between oxygen atoms ($r = r_{\text{first neighbor}}$). We observe that two kinds of motion are present: the usual continuous diffusive motion which is characterized by a widening of the Van Hove function with time and a continuous shift of the maximum of $4\pi r^2 G_s(r,t)$ to larger r values. Also, the hopping motions which are characterized by an increase of the Van Hove for $r = r_{\text{first neighbor}}$ lead to the appearance of a bump at this distance and a simultaneous decrease of the first peak. We observe in Figure 4 that the continuous lines curves for $r < 2$ Å display larger shifts to large r values

showing that the continuous flow motion is more important for large boxes than for small boxes. We also observe that the bump for $r = r_{\text{first neighbor}}$ is roughly the same for the two different boxes. This result suggests that the hopping motions are less affected by the system size than the sluggish heterogeneous dynamics which is in turn deeply affected. This result may explain the association of an increase of the non-Gaussian parameter with a decrease of the dynamical aggregations.

Conclusion

We have studied finite size effects on dynamical heterogeneity in liquid silica with Molecular Dynamics simulations using the BKS potential model. When the system size decreases relaxation times are found to increase in accordance with previous results in finite-size simulations and confined liquids. It has been suggested that this increase may be related to a modification of the spatially heterogeneous dynamics in confined liquids. In agreement with this hypothesis we observe a decrease of the dynamical heterogeneities associated with the most and the least mobile atoms when the size L decreases. However, we find that the decrease of the dynamical aggregation associated with the least mobile atoms is much more important than the decrease associated with the most mobile atoms. This result associated with a slowing down of the liquid is surprising. The decrease of the heterogeneous behaviour is also in contradiction with the increase of the heterogeneities observed in liquids confined in some nanopores. However an increase of the non-Gaussian parameter appears both in nanopores and in the finite size simulations. As the non-Gaussian parameter is usually associated with dynamical heterogeneities, the increase of the non-Gaussian parameter together with a decrease of dynamical heterogeneity is also surprising. This result seems to eliminate dynamical heterogeneity as the unique cause for the non-Gaussian behaviour of glass-forming liquids. Care should be taken when using the non-Gaussian parameter as a measure of the heterogeneity in glass-forming liquids.

References

1. G. Adam, J.H. Gibbs, J. Chem. Phys. **43**, 139 (1965)
2. M.D. Ediger, Annu. Rev. Phys. Chem. **51**, 99 (2000)
3. H. Sillescu, J. Non-Crystal. Sol. **243**, 81 (1999)
4. W. Kob, C. Donati, S.J. Plimpton, P.H. Poole, S.C. Glotzer, Phys. Rev. Lett. **79**, 2827 (1997)
5. C. Donati, J.F. Douglas, W. Kob, S.J. Plimpton, P.H. Poole, S.C. Glotzer, Phys. Rev. Lett. **80**, 2338 (1998)
6. R. Yamamoto, A. Onuki, Phys. Rev. Lett. **81**, 4915 (1998)
7. R. Yamamoto, A. Onuki, Phys. Rev. E **58**, 3515 (1998)
8. A. Kerrache, V. Teboul, D. Guichaoua, A. Monteil, J. Non-Cryst. Solids **322**, 41 (2003)
9. V. Teboul, C. Alba-Simionesco, Chem. Phys. **317**, 245 (2005)
10. V. Teboul, A. Monteil, L.C. Fai, A. Kerrache, S. Maabou, Eur. Phys. J. B **40**, 49 (2004)
11. M. Vogel, S.C. Glotzer, Phys. Rev. E **70**, 061504 (2004)
12. V. Teboul, S. Maabou, L. C. Fai, A. Monteil, Eur. Phys. J. B **43**, 355 (2005)
13. V. Teboul, C. Alba-Simionesco, J. Phys.: Cond. Matt. **14**, 5699 (2002)
14. C. Alba-Simionesco, G. Dosseh, E. Dumont, B. Frick, B. Geil, D. Morineau, V. Teboul, Y. Xia, Eur. Phys. J. E **12**, 19 (2003)
15. P. Scheidler, W. Kob, K. Binder, Europhys. Lett. **52**, 277 (2000); P. Scheidler, W. Kob, K. Binder, Europhys. Lett. **59**, 701 (2002); P. Scheidler, W. Kob, K. Binder, Eur. Phys. J. E **12**, 5 (2003)
16. F. Varnik, J. Baschnagel, K. Binder, M. Mareschal, Eur. Phys. J. E **12**, 167 (2003); F. Varnik, J. Baschnagel, K. Binder, Eur. Phys. J. E **8**, 175 (2002)
17. K. Kim, R. Yamamoto, Phys. Rev. E **61**, R41 (2000)
18. Z. Yigang, G. Guangjun, K. Refson, Z. Yajuan, J. Phys.: Cond. Matt. **16**, 2427 (2004)
19. J. Horbach, W. Kob, K. Binder, C.A. Angell, Phys. Rev. **54**, R5897 (1996)
20. B. Doliwa, A. Heuer, J. Phys.: Cond. Matt. **15**, S849 (2003)
21. J. Horbach, W. Kob, K. Binder, Eur. Phys. J. B **19**, 531 (2001)
22. M.P. Allen, D.J. Tildesley, *Computer simulation of liquids* (Oxford University Press, New York, 1990)
23. B.W.H. Van Beest, G.J. Kramer, R.A. Van Santen, Phys. Rev. Lett. **64**, 1955 (1990)
24. Y. Guissani, B. Guillot, J. Chem. Phys. **104**, 7633 (1996)
25. M. Hemmati, C.A. Angell, *Physics meets geology*, edited by M. Aoki, R. Hemley (Cambridge University Press, 1998)
26. A. Kerrache, V. Teboul, A. Monteil, Chem. Phys. **321**, 69 (2006)
27. J.C. Mikkelsen, Appl. Phys. Lett. **45**, 1187 (1984)
28. G. Brebec, R. Seguin, C. Sella, J. Brevenot, J.C. Martin, Acta. Mettall. **28**, 327 (1980)
29. H.J.C. Berendsen, J.P.M. Postma, W. Van Gunsteren, A. Di Nola, J.R. Haak, J. Chem. Phys. **81**, 3684 (1984)
30. C. Bennemann, C. Donati, J. Baschnagel, S.C. Glotzer, Nature **399**, 246 (1999)
31. M. Goldstein, J. Chem. Phys. **51**, 3728 (1969)
32. J. Horbach, W. Kob, K. Binder, Phil. Mag. B **77**, 297 (1998)